Adsorption of Gas-Phase Nitric Acid to *n*-Hexane Soot: Thermodynamics and Mechanism

Daniel G. Aubin and Jonathan P. Abbatt*

Department of Chemistry, University of Toronto, 80 St. George St., Toronto, ON, Canada M5S 3H6

Received: July 18, 2003; In Final Form: September 29, 2003

The adsorption of gas-phase nitric acid on *n*-hexane soot was measured as a function of temperature, relative humidity (RH), and nitric acid partial pressure in a coated-wall flow tube coupled to an electron-impact mass spectrometer. The specific surface area (SSA) of the soot, determined from the BET isotherm of Kr at 77 K for each sample, was 88−372 times larger than the geometric surface area. The SSA increased linearly with soot mass for thin samples but saturated at high mass. For the most part, the nitric acid adsorption was reversible in the submonolayer regime, and no indication of HONO formation was observed. The uptake increased with decreasing temperature and, for surface coverages between 10^{12} and 10^{13} molecules cm^{-2}, the average enthalpy of adsorption was -55.8 ± 7.7 kJ mol^{-1}. A Langmuir−Freundlich model with the heterogeneity parameter equal to 0.5 closely describes the uptake data, implying either that the surface sites are energetically heterogeneous or that nitric acid is dissociating on the surface. The nitric acid adsorption isotherms were independent of relative humidity up to 80% RH at 243 K. Exposure to ppm levels of ozone for about 1 h had no effect on the adsorption. The atmospheric implications of this work are discussed.

1. Introduction

Soot aerosol particles form from the incomplete combustion of carbonaceous fuels and have an average global source estimated to be as high as 24 Tg yr^{-1}.[1,2] They have been observed to comprise tens of percent of the total aerosol carbon in both rural and urban areas.[3−5] Carbonaceous aerosols have large optical absorption coefficients, which leads them to have a significant impact on Earth's radiative balance by absorbing both incoming solar radiation and outgoing infrared radiation.[6] They may also act as cloud condensation nuclei (CCN).[7] In particular, the adsorption of water-soluble species such as H_2SO_4 and HNO_3 is thought to facilitate the activation of soot particles as CCN.[8−10]

Heterogeneous chemistry occurring on black carbon may also affect atmospheric levels of trace gases such as SO_2, O_3, and NO_x species. In particular, since these particles represent a chemically reducing substrate in an oxidizing atmosphere, it has been suggested that there is a heterogeneous reaction converting HNO_3 to NO_x.[11,12] This could impact O_3 formation rates and help explain why some models have $[HNO_3]/[NO_x]$ ratios that are 5−10 higher than those found by ambient measurements,[12,13] although new gas-phase kinetics measurements may be able to account for some of this discrepancy. [14] Similarly, there is evidence that interactions of NO_x with soot give rise to HONO, a potent OH source.[15] These reactions have the potential to be atmospherically significant, given the high levels of soot in urban air and that the specific surface area of soot in the upper troposphere and lower stratosphere may be similar to that of sulfuric acid during volcanically quiescent periods.[16]

There remain large uncertainties in assessing the chemical effects of carbonaceous aerosols in the atmosphere for a number of reasons. In particular, in laboratory studies a wide variety of different carbonaceous substrates have been used: hydrocarbon soot from methane,[17] propane,[17] hexane,[18−20] and decane;[11] soot from fuels such as diesel[19] and kerosene;[17,18] amorphous carbon[18−21] and graphite spark-generated soot.[19,22] In addition, there is a particular lack of knowledge about the specific surface area and the surficial chemical composition of carbonaceous materials used in laboratory studies as well as in the atmosphere. Last, the results from some laboratory studies of trace gas interactions may not be applicable, since the experiments were performed at particularly high, non-atmospherically relevant partial pressures.

In the specific case of nitric acid, some studies demonstrated that a reactive interaction proceeds efficiently, which leads to the formation of NO_x, i.e., both NO and NO_2, along with other species such as H_2O.[21,23] One characteristic of these studies is that high surface coverages of nitric acid must have been prevalent given the high partial pressures employed. Two other studies, both employing coated-wall flow tubes, found little evidence for a reactive interaction when the partial pressures were kept low.[16,17] Indeed, the study of Choi and Leu[18] showed that substantial irreversible loss of nitric acid proceeds if the partial pressures are higher than 10^{-4} Torr on amorphous black carbon and graphite soot surfaces, but reversible uptake describes the behavior at lower partial pressures. In addition, at high partial pressures, they report that the reactive process requires an initiation period before products were observed, which probably represents the time required for sufficient surface coverages of nitric acid to develop. Additional studies have confirmed this low reactivity.[19,20,22] For example, it was shown using FT-IR spectroscopy to monitor the chemical state of the soot substrate that irreversible modification of the soot does occur at fairly low partial pressures ($\approx 10^{-4}$ Torr) but with long-term uptake coefficients of roughly 10^{-6}.[19] Similarly, a smog chamber study conducted on time scales of a few days showed that the reactive uptake coefficient for loss of nitric acid was less than 10^{-7}.[22] These small uptake coefficients are not easily measured in coated-wall flow tube systems. Most recently, a study of the interaction of nitric acid with a decane-soot surface formed from a fuel-rich flame reported very high yields for the

* Corresponding author. E-mail: jabbatt@chem.utoronto.ca.

10.1021/jp036105g CCC: $25.00
Published on Web 11/15/2003

production of HONO, with steady-state reactive uptake coefficients of 5×10^{-4}.[11]

An uncertainty that pertains to these studies is that the specific surfaces areas of the samples under consideration were not measured directly. Instead, BET surface areas, either measured or taken from the literature, of similar powder samples were used. From an atmospheric modeling perspective, uncertainties also arise because the temperature dependence of the nitric acid uptake has not been well established, having only been investigated once, at 220, 295, and 503 K.[18] Similarly, the effect of atmospherically relevant relative humidities (RH) has only been examined once, at 50% RH,[22] even though it is known that RH affects the soot heterogeneous chemistry of reactive nitrogen species[24] and the uptake of semivolatile organics species to aerosols.[25−27] Last, the effect of surface oxidation on the uptake of nitric acid has not been investigated, even though this has been shown to influence the extent of the adsorption of water on hexane soot.[28]

Given that there is now considerable evidence that under relevant atmospheric partial pressure conditions, the uptake of nitric acid to hydrocarbon soot occurs primarily via a nonreactive, reversible process, we have undertaken systematic adsorption studies of nitric acid to hexane soot. The motivation is to assess the mechanism of the adsorption process and to better determine whether physical scavenging by soot will have significant effects on atmospheric levels of gas-phase nitric acid. Hexane soot was used as a proxy for carbonaceous aerosols, since it contains both elemental carbon and organic carbon and its structure and physical properties have been extensively studied.[28−32] We have performed the studies over a wide range of relatively low nitric acid partial pressures and at atmospherically relevant temperatures and relative humidities. For the first time, we have measured the BET specific surface area (SSA) for each sample used so as to obtain a more representative value of the accessible surface area. Finally, the soot surfaces were exposed to ozone to gauge the potential effects of atmospheric "aging".

2. Experimental Section

The uptake experiments were conducted in a low pressure, coated-wall flow tube coupled to an electron-impact mass spectrometer similar to that used previously to measure the adsorption of gases onto thin films of ice.[33] Briefly, soot produced from an *n*-hexane flame from an alcohol burner, provided with an air flow of 10−13 SLPM, was evenly deposited on the inner walls of a 22 cm long, 2.3 cm i.d. Pyrex tube held 5−10 cm above the tip of the burner. The soot was deep black and the mass deposited ranged from 0.0076 to 0.3787 g, covering a geometric surface area of 158 cm^2. The SSA of the soot samples was determined by measuring the BET adsorption isotherm of Kr on the soot sample at 77 K.[34] This was achieved by exposing the soot-coated Pyrex tube, housed in a 22 cm long, 3 cm i.d. stainless steel cylinder equipped with copper gasket seals and immersed in liquid nitrogen, to different known amounts of Kr. The number of moles of Kr adsorbed to the soot surface was obtained from the difference in the final pressure after exposing the soot sample to Kr and that which would have been obtained from the expansion of the Kr into an empty chamber. The final pressure was then measured with a capacitance manometer (MKS Instruments Inc., Model 122AA-0010AD). The surface area was then determined from the linearized form of the BET isotherm using the method recommended by IUPAC.[35]

To perform an uptake experiment the soot-coated tube was inserted into a double-jacketed flow tube through which a flow of 419−449 sccm of a helium carrier gas (high purity grade, Air Products) at 0.77 Torr was established for 10−15 min prior to beginning an experiment. When a humidified carrier gas was required, a portion of the helium was diverted through a bubbler containing doubly distilled deionized water. The flow and pressure of helium entering the bubbler was measured with a mass flow meter (MKS Instruments Inc., Model 0258C-020005V) and a 10 Torr full scale capacitance manometer (MKS Instruments Inc., Model 122AA-00010AD), which allowed for a precise determination of the relative humidity in the flow tube. The uptake experiments were conducted from 228 to 295 K by using a low-temperature circulating bath (Neslab, Model ULT-80).

A differentially pumped electron-impact mass spectrometer (UTI) sampled the composition of the gas exiting the flow tube by monitoring in single-ion mode mass 46 for HNO_3 and mass 47 for HONO.[36] The detection limits for nitric acid were between 10^{-7} and 10^{-6} Torr. Nitric acid was added to the flow tube through a movable injector initially positioned with its tip beyond the downstream end of the soot film. Before each experiment the system was passivated with HNO_3 for 20−30 min to obtain a stable signal. In all cases, the flow exiting the injector tip never exceeded 10% of the total flow in the flow tube, which ensured that mixing into the bulk flow was rapid. The partial pressure of the nitric acid in the flow tube was determined from the pressure drop with time from a glass reservoir containing nitric acid diluted in helium. The mixture of nitric acid in helium was made by drawing on the headspace of a 3:1 mixture of 96% H_2SO_4 and 68−70% HNO_3 (Fischer Scientific) that had been purified of air by three successive freeze−pump−thaw cycles.

The uptake experiments were conducted by pulling the injector back over the soot film by a distance of either 5, 10, or 20 cm, the exact value being determined by the need to see a sufficiently large change in signal indicative of partitioning to or reaction with the surface. The injector was then pushed back to the starting position after the signal from the mass spectrometer had approached a steady-state value. The loss of signal after withdrawing the injector was integrated to determine the amount of nitric acid lost to the surface, where a criterion of 85% signal recovery was used to determine the point at which the surface was saturated. By referencing this amount to the surface area exposed, an uptake (or surface coverage) is obtained.[37]

For the oxidation experiments, ozone was prepared by photolyzing oxygen (Air Products, Extra Dry Grade) flowing through a cell irradiated with a UV lamp at 185 nm (Jelight Company Inc., Model 100). To trap the ozone, the resulting mixture of oxygen and ozone was flowed through a bed of silica gel immersed in ethanol that had been cooled with liquid nitrogen. The ozone was then transferred to a bulb by pumping on the headspace above the silica. The concentration of the ozone in the bulb was determined by measuring the absorbance at 254 nm.

3. Results and Discussion

A. Specific Surface Area. Experimental adsorption isotherms for Kr on a soot film at 77 K are typical of a type II isotherm, as identified by Brunauer, Emmett and Teller, which arise from physical adsorption with multilayer formation (see Figure 1).[34]

The knee of the isotherm (at $p/p^\circ \approx 0.2$ in Figure 1), referred to as the B point, can be taken as the point of completion of a monolayer. By knowing the number of moles required to form a monolayer and the cross-sectional area of the adsorbate gas, the surface area can be obtained.

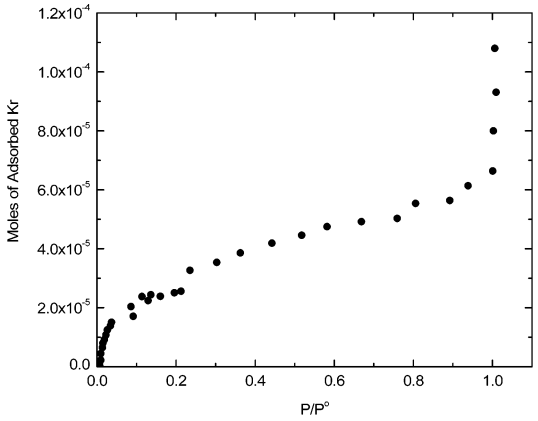

Figure 1. BET isotherm for the adsorption of Kr on soot at 77 K for a 0.0561 g sample with a specific surface area of 2.4 ± 0.1 m^2.

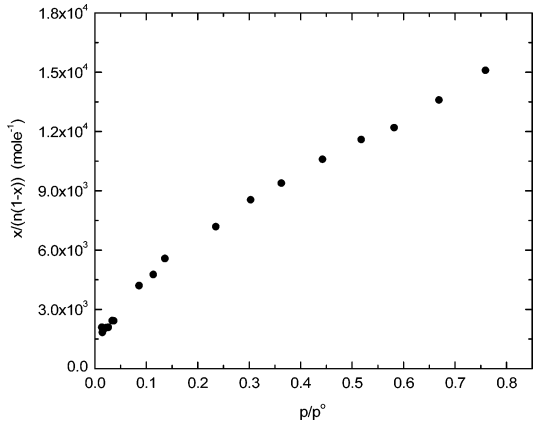

Figure 2. Linearized form of the BET isotherm for the adsorption of Kr on soot at 77 K for a 0.0561 g sample with a specific surface area of 2.4 ± 0.1 m^2 ($x = p/p°$, where p is the partial pressure and $p°$ is the saturation vapor pressure, and n is the number of moles of Kr adsorbed on the soot sample).

A more accurate method to determine the surface area is to fit the adsorption isotherm to the linearized form of the BET equation:[34]

$$\frac{p/p°}{n(1 - p/p°)} = \frac{1}{n_m C} + \frac{C - 1}{n_m C}(p/p°) \qquad (1)$$

where p is the pressure of the gas above the surface, $p°$ is the saturation vapor pressure of the gas at the temperature used, n is the number of moles adsorbed, n_m is the monolayer capacity (i.e., the number of moles of the adsorbate in a monolayer), and C is a constant. By plotting the left-hand side of eq 1 versus $p/p°$ (see Figure 2), one should obtain a straight line, generally within the range of $p/p°$ of 0.05−0.35.[35]

The slope $s = (C - 1)/n_m C$ and intercept $i = 1/n_m C$, can be rearranged to yield the monolayer capacity $n_m = 1/(s + i)$.[35] The surface area, a(BET), is then obtained from

$$a(\mathrm{BET}) = n_m N_A \sigma_{Kr} \qquad (2)$$

where N_A and σ_{Kr} are Avogadro's number and the cross-sectional area of a Kr atom (generally taken to be 0.202 nm^2),[38] respectively.

The surface areas obtained from the B point method and the linearized BET isotherm agreed within 20% of each other. However, the surface areas quoted hereafter were all obtained from the linearized BET isotherm, since this method is less arbitrary. Figure 3 shows the experimentally determined surface areas for a series of soot samples as a function of sample mass.

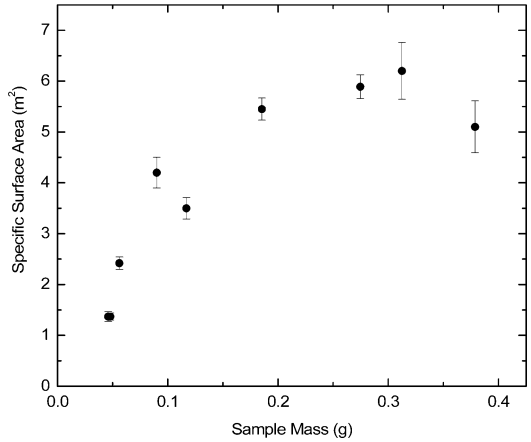

Figure 3. Specific surface area of the soot samples as a function of mass as determined from the linearized BET isotherm.

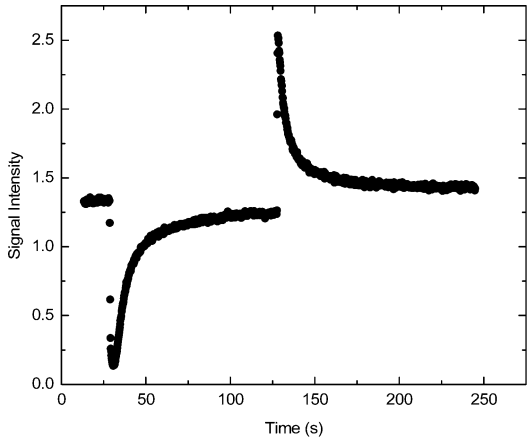

Figure 4. Mass spectrometer signal as a function of time for the uptake of nitric acid on a 0.0901 g soot sample with a specific surface area of 4.2 ± 0.3 m^2 at 283 K with a nitric acid partial pressure of 5.9 × 10^{-5} Torr.

It was found that the specific area was 88−372 times larger than the geometric surface area of the soot sample. Figure 3 shows that there is not a corresponding increase in surface area with sample mass beyond a certain point. This is consistent with previous Knudsen cell kinetic studies, which measured uptake coefficients of nitrogen oxides on mineral dust that increased linearly with sample mass at low sample masses but then leveled off for larger sample masses.[39] The explanation for our observations (and those in the Knudsen cell work) is that at larger soot masses only the top portion of the sample is being probed by the Kr. Previous studies have referenced their results to BET surface areas quoted by the manufacturer, given as area per unit mass, or else, only a rough estimate has been given. Given the results in Figure 3, the SSA's used in some studies may have been smaller than thought, especially if large sample masses were used.

B. Nitric Acid Adsorption. A typical uptake profile for nitric acid on soot, at 283 K, is shown in Figure 4. The initial drop in the signal corresponds to pulling the injector back, thus exposing the soot sample to the nitric acid, which then partitions to the surface. Pushing the injector back to the start position leads to the observed increase in the signal, because the nitric acid desorbs from the soot. The adsorption and desorption areas are similar to each other, to within at least 20%, and repeated uptakes at equal pressures on the same film yielded uptake areas

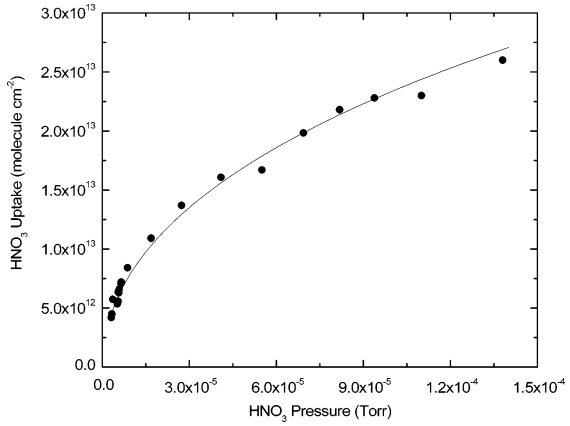

Figure 5. Nitric acid adsorption isotherm on soot for a 0.1169 g sample with a specific surface area of 3.5 ± 0.2 m^2 at 283 K fit to the Langmuir−Freundlich isotherm with $\nu = 0.5$ and $K = 38 \pm 1$ $Torr^{-1}$.

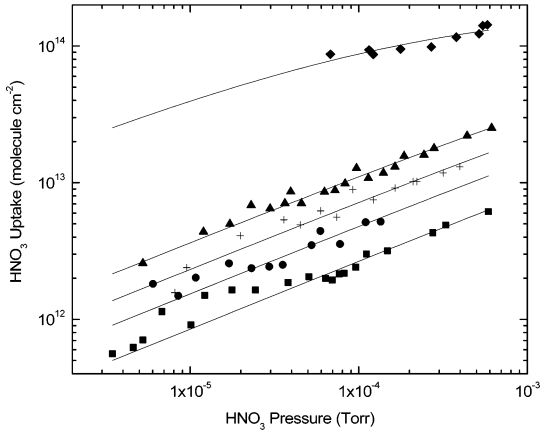

Figure 6. Nitric acid adsorption isotherm for soot on a 0.0901 g sample with a specific surface area of 4.2 ± 0.3 m^2 fit to the Langmuir−Freunlich isotherm with $\nu = 0.5$ at various temperatures (squares = 295 K, circles = 283 K, crosses = 273 K, triangles = 263 K, and diamonds = 228 K).

that had a precision of ±15%. In runs where the desorption was observed over a long time scale, the areas were very similar, with agreement to within 10% or so, with the desorption peak usually smaller than the adsorption peak. From these observations it was clear that a very large fraction of the uptake was reversible.

From a temporal perspective, there is a short-term component of the uptake, where the nitric acid signal rapidly decreases and then increases, which is followed by a long term component (e.g. after 75 s in Figure 4), where the nitric acid signal slowly recovers back to its initial level. This long-term component may be due to slow diffusion of the nitric acid into the underlying layers and pores of the soot film. The rapid surge in the signal after pushing back the injector indicates that the desorption lifetime for nitric acid from the soot is less than the time required to push the injector back, i.e., on the order of a second. This suggests that the soot surface readily reaches equilibrium with the gas-phase nitric acid over the exposure time scales used.

Figure 5 shows a typical adsorption isotherm for HNO_3 on soot obtained at 283 K. As expected, the uptake increases as the partial pressure of HNO_3 is increased. To help determine the nature of the adsorption mechanism, the experimental data were fit to a variety of adsorption isotherms. A very good fit is obtained with the Langmuir−Freundlich isotherm[40]

$$\frac{\theta}{\theta_m} = \frac{(KP)^\nu}{1 + (KP)^\nu} \tag{3}$$

where θ is the surface coverage; θ_m is the surface coverage for a monolayer, which we take to be 2×10^{14} molecules cm^{-2} (see below); P is the partial pressure of the adsorbate gas over the surface; K is the gas−surface equilibrium constant; and ν is a heterogeneity parameter. The Langmuir isotherm, where it is assumed that all sites are equivalent and the ability of the molecule to bind is not affected by the occupation of neighboring sites, does a poor job of fitting the data. Addition of the heterogeneity parameter, ν, in the Langmuir−Freundlich isotherm takes into account the presence of adsorption sites with different binding energies.[40] As ν tends to 1 the surface becomes more homogeneous until eq 3 becomes the Langmuir isotherm when ν equals unity.

For the experimental data the Langmuir−Freundlich isotherm provided a good fit (see Figure 5) with a consistent value of ν close to 0.495 ± 0.065 for all the films. This value for the heterogeneity parameter is significant, since a mechanism involving adsorption followed by reversible dissociation on the surface will be described by the Langmuir−Freundlich equation with $\nu = 0.5$.[41] In this case, the isotherm is more commonly referred to as the dissociative Langmuir isotherm. This is the first evidence that we are aware of that suggests that nitric acid could be reversibly dissociating on a soot surface.

It should be noted that the Freundlich isotherm, where a and n are empirical parameters, also gives a reasonable fit to most of the experimental data:[41]

$$\theta = aP^{1/n} \tag{4}$$

However, our preference in using the Langmuir−Freundlich model is that there was evidence for surface saturation in the absorption isotherms at high surface coverages, achieved by using low temperatures and high nitric acid partial pressures, e.g. at 228 K and 3×10^{-4} Torr of nitric acid in Figure 6.

For these conditions, partial saturation of the surface was found to occur at values close to $\approx 10^{14}$ molecules cm^{-2}. This specific surface coverage is significant because 2×10^{14} molecules cm^{-2} corresponds roughly to the formation of a complete monolayer for molecules of the size of nitric acid, suggesting that there is no multilayer adsorption taking place at this point. Indeed, saturated surface coverages of 2×10^{14} molecules cm^{-2} have been measured for HNO_3 on ice surfaces.[37] Note that the Langmuir−Freundlich model predicts that surface saturation will occur, whereas the Freundlich model does not.

The only other study in the literature where the adsorption isotherm of nitric acid to soot has been measured is that of Choi and Leu.[18] Also using hexane soot, these workers see a clear partial pressure dependence to their uptakes and evidence of surface saturation at partial pressures near 3×10^{-4} Torr of nitric acid at 295 K. Comparing this study to our results, we are well in the submonolayer regime and see no evidence for surface saturation under these high-temperature conditions. Choi and Leu[18] use a Langmuir model to fit their data, although only four points are included in the fit, whereas we find the Langmuir model does a poor job of fitting our data. Previous work done on the uptake of SO_2 and NH_3 on *n*-hexane soot has shown that the adsorption isotherms were better modeled by a sum of different Langmuir isotherms—which is essentially equivalent to the use of a Langmuir−Freundlich equation—each one representative of a particular type of adsorption site.[42,43] However, as mentioned in the Summary section, these data for SO_2 uptake are also extremely well fit by a dissociative

Langmuir isotherm, i.e., a Langmuir−Freundlich model with a heterogeneity parameter equal to 0.5.

It should be noted that the reversibility of the uptake for nitric acid was found to depend on the manner by which the hexane soot film was prepared. For all the results presented so far (and for those in sections C−E), the flame was kept well away from the soot deposition region. If the flame was allowed to come in contact with the soot deposited on the Pyrex tube, then the observed uptake was no longer fully reversible. Quite frequently, the signal recovered to a steady-state value below the initial value, for example to 91% of its initial value when the injector was withdrawn 10 cm, corresponding to a steady-state uptake coefficient of 1.2×10^{-3} at 295 K for 2.7×10^{-5} Torr of HNO_3. In one particular case, when high surface coverages of nitric acid developed at 228 K and 5×10^{-5} Torr of nitric acid, there was a pronounced loss of nitric acid for which an uptake coefficient of $\gamma = 2.8 \times 10^{-3}$ was calculated. This was a steady-state loss over an observation period of 100 s, during which there was no observed change in the level of reactivity. We were unable to reproduce this pronounced reactive behavior in other soot films formed by allowing the flame to come in contact with the soot deposited on the inside of the Pyrex tube.

Note that the uptake coefficients, γ, just quoted were calculated from eq 5 and using the geometric surface area of the soot film

$$\gamma = \frac{2rk}{\omega} \tag{5}$$

where r is the radius of the flow tube, k is the first-order loss rate coefficient, and ω is the mean thermal speed of the reactant.[44] k is determined in the standard manner by measuring the nitric acid signal as a function of injector distance in the flow tube. The correction for gas-phase diffusion to the wall is small for uptake coefficients of this magnitude and, given that kinetics is not the focus of this work, we do not attempt to correct for the roughness of the film.

The observed steady-state uptake was probably due to the flame activating the soot in some manner over the time during which the soot was collected. We highlight these observations to illustrate how the nature of the interaction between nitric acid and soot may be significantly altered from the largely reversible behavior observed at low surface coverages, i.e., that which is the primary focus of this paper. In particular, high partial pressures, well beyond atmospheric levels, and/or flame-activation of the soot may lead to irreversible loss of the nitric acid. We note that in this work we were unable to monitor the formation of NO or NO_2, since they share the same ion signals as nitric acid, namely m/z 30 and 46. To circumvent this would have required monitoring nitric acid at m/z 63, which is a significantly weaker signal.

The prevalence of a reactive process at high partial pressures is in accord with the findings of other researchers, where NO_2 and NO were formed as the main products.[11,18−21,23] For example, Choi and Leu have invoked a bimolecular decomposition mechanism to explain their observation of nitric acid decomposition at high nitric acid partial pressures leading to the formation of NO_2, NO, H_2O, and unidentified volatile products.[18] It is also important to note that Salgado Munoz and Rossi have observed the formation of HONO with yields of up to 50% when decane soot, prepared from a fuel rich flame, was exposed to nitric acid.[11] Accordingly, we monitored the mass 47, i.e., $HONO^+$, during several uptake experiments on different films that had been processed by the flame, but we observed no increase in the signal above the background level, even with high surface coverages of nitric acid. However, we should point out that this is only a preliminary assessment of whether HONO is indeed formed. Although Rossi and co-workers have reported detection of HONO as $HONO^+$ using electron-impact mass spectrometry,[36] without a calibrated source of HONO we are uncertain of the degree to which HONO yields its parent ion in our electron-impact MS.

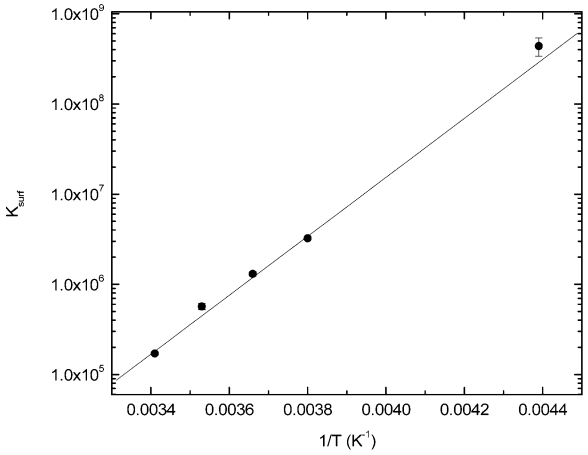

Figure 7. van't Hoff plot of the experimental gas-to-surface equilibrium constant K_{surf} for the adsorption of nitric acid on a 0.0901 g sample with a specific surface area of 4.2 ± 0.3 m^2 using the equilibrium constants obtained from the Langmuir−Freundlich isotherm with $\nu = 0.5$ fit to the data in Figure 6.

C. Nitric Acid Adsorption Thermodynamics. We report detailed nitric acid adsorption experiments from room temperature to 253 K for three films and down to 228 K for a fourth film. As expected, the uptake of nitric acid and the time required to saturate the soot surface increased as the temperature was lowered (see Figure 6, for example). For a constant nitric acid partial pressure, the shape of the uptake profile also changed with temperature, since more time was required to saturate the surface at lower temperatures. This caused the overall uptake profile to appear more rounded at lower temperatures. Since temperature-dependent values of the equilibrium constant, K, were obtained from the Langmuir−Freundlich isotherm, we could extract an enthalpy of adsorption, $\Delta H_{ads}^{vantHoff}$, for nitric acid on soot from a standard van't Hoff plot as defined from eq 6.

$$\Delta H_{ads}^{vantHoff} = -R\left(\frac{\partial(\ln K)}{\partial(1/T)}\right) \tag{6}$$

Figure 7 shows the resulting graph obtained from eq 6 for one soot film, i.e., using the data in Figure 6.

To obtain a unitless equilibrium constant in the van't Hoff plot, K_{surf}, we have referenced the equilibrium constant obtained from the Langmuir−Freundlich isotherm to the standard state of Kemball and Rideal for a molecule adsorbed onto a surface in terms of volume per molecule.[45] At 273 K, assuming that the average volume per molecule is 36 930 Å^3, this gives a standard state of 1.6×10^{12} molecules cm^{-2}, roughly 1% of a monolayer.

An isosteric heat of adsorption, $\Delta H_{ads}^{isosteric}$, was calculated from the fit of the Freundlich isotherm to the data:[46]

$$\Delta H_{ads}^{isosteric} = R\left(\frac{\partial(\ln P)}{\partial(1/T)}\right)_{\theta} \tag{7}$$

In this case, the heat of adsorption was obtained from the slope of the plot of ln P vs T^{-1} for a specific surface coverage,

TABLE 1: Heats of Adsorption of HNO_3 to *n*-Hexane Soot Obtained from the Langmuir−Freundlich and Freundlich Isotherms

soot film area (m^2)	$\Delta H_{ads}^{vantHoff}$ (kJ $mole^{-1}$)	$\Delta H_{ads}^{isosteric}$ (kJ $mole^{-1}$)
1.37 ± 0.12	-58.8 ± 8.8	-58.2 ± 8.7
3.5 ± 0.2	-53.6 ± 1.6	-53.1 ± 1.1
4.2 ± 0.3	-64.5 ± 2.7	-55.5 ± 3.1
5.9 ± 0.2	-46.5 ± 5.4	-44.3 ± 6.5
average	-55.8 ± 7.7	-52.8 ± 6.0

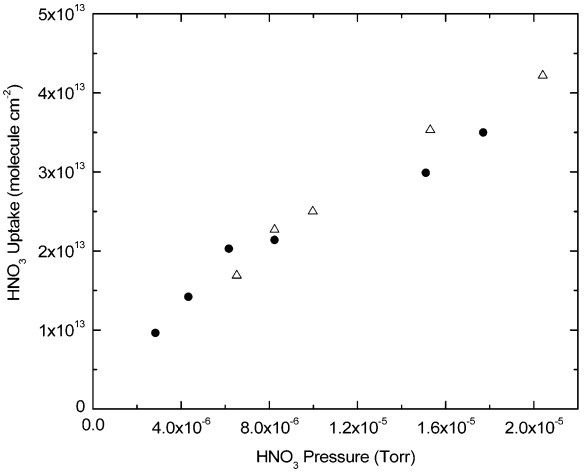

Figure 8. Nitric acid uptake on a 0.1169 g soot sample with a surface area of 3.5 ± 0.2 m^2 at 253 K with dry a carrier gas (circles) and with a humidified carrier gas with a relative humidity of 27% (triangles).

which was within a factor of 2 of 1×10^{13} molecule cm^{-2} for all films. The pressure of nitric acid required to obtain this surface coverage was calculated from the Freundlich isotherm fit to the data. Table 1 lists the enthalpies of adsorption that were obtained for four different soot films using the two approaches.

The adsorption energies measured by both the van't Hoff and isosteric approaches are higher than the -21 kJ $\pm$ 1 mol^{-1} adsorption enthalpy for NH_3 on hexane soot measured by Muenter and Koehler[42] and the value of -26 ± 4 kJ mol^{-1} for SO_2 on hexane soot measured by Koehler et al.[43] If the molecules are binding to specific polar functional groups on the soot surface, then one would expect the adsorption energies to scale with the relative polarities and the dipole moments of the molecules. This is what is observed as the dipole moments for HNO_3, SO_2, and NH_3 are 2.17, 1.6, and 1.47 D, respectively.[47]

D. Uptake Dependence on Relative Humidity. The uptake experiments were also performed as a function of relative humidity. To keep the overall pressure in the flow tube in the plug flow regime, the highest relative humidities were achievable at cold temperatures. In particular, we could reach 80% RH at 243 K, and a number of experiments were also done at higher temperatures (and lower RH). Within the precision of the experiments, which is on the order of $\pm$10%, the humidified carrier gas had no discernible effect on the uptake of nitric acid on soot. An example of adsorption isotherms measured with and without water vapor in the flow is shown in Figure 8.

From measurements of the surface residence time of water on *n*-hexane soot from a fuel-rich flame, Alcala-Jornod et al. have determined the surface density of water adsorption sites to be $(3 \pm 1) \times 10^{13}$ sites cm^{-2} between 298 and 243 K.[48] Given this fairly low surface density of adsorbed water, it is probably not surprising that there is little effect on the levels of adsorbed nitric acid. The adsorption thermodynamics also

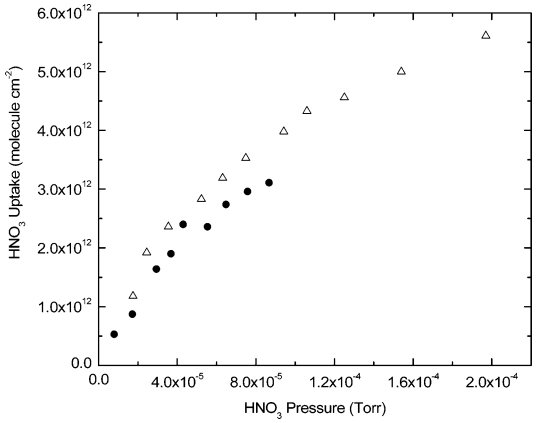

Figure 9. Nitric acid uptake on soot before ozonation (circles) and after ozonation (triangles) with 1−2 ppm of ozone for 55 min on a 0.0479 g sample with a specific surface area of 1.37 ± 0.12 m^2.

suggest that the nitric acid is not dissolving into a multilayer-thick film of water on the soot surface. In particular, the experimental adsorption enthalpy, -55.8 kJ mol^{-1} on average, is significantly lower than the enthalpy of dissociation of -71.1 kJ mol^{-1} for gas-phase nitric acid dissolving into water: HNO_3-(g) $\rightarrow H^+$(aq) + NO_3^- (aq).[41] This implies that the degree of ion hydration present in liquid water is greater than that occurring on the soot surface, if dissociation is indeed occurring.

E. Ozonation Experiment. Two separate soot films were ozonated with 1−2 ppm of ozone for 45 and 55 min, respectively. Relative to the unoxidized films, no increase was observed in the uptake of nitric acid at room temperature on the film ozonated for 45 min, and a negligible increase (<15%) was seen for the film ozonated for 55 min (see Figure 9). Note that we performed some other experiments at very high levels of ozone of a few tenths of a percent, and nonreproducible results were obtained. In one case, a significant enhancement of close to an order of magnitude was observed, but in three others the nitric acid uptake did not increase within the experimental uncertainties.

The negligible increase in adsorption seen in the films treated with ppm levels of ozone is somewhat surprising, since the oxidation of the surface is expected to render it more oxygenated and to lead to an increase in the adsorption of polar species such as nitric acid. However, this negligible effect could be due to a low density of surface reactive sites available to ozone, consistent with the relatively small reactive uptake coefficients that have been measured for ozone on soot.[17,49,50] For the films treated with ppm levels of ozone, the fit to the Langmuir−Freundlich isotherm was similar before and after ozonation, suggesting there was no change in the adsorption mechanism.

4. Summary

A. Adsorption Mechanism. From the experimentally determined heat of adsorption, -55.8 ± 7.7 kJ mol^{-1} on average, it can be deduced that condensation onto the soot surface is not the driving force for adsorption, since the heat of condensation for nitric acid, which is -39.1 kJ mol^{-1},[47] is lower than the heat of adsorption. However, the heat of adsorption is not as large as that arising from dissolution into water, followed by dissociation into hydrated ions, i.e. -71.1 kJ/mol.[41]

At this point, two models can describe the full adsorption mechanism. In the first, given the structure of nitric acid, with three electronegative oxygen atoms and an electropositive hydrogen atom, it seems likely that it can strongly hydrogen bond to the soot surface. The formation of two or three hydrogen

bonds, with roughly a strength of 20 kJ mol^{-1} each,[41] would be consistent with our experimental heats of adsorption. Indeed, Akhter et al. have shown that the surface of hexane soot contains many carbon−oxygen functionalities such as carbonyls, ethers, hydroxyls, carboxylic acids, and acids anhydrides, which could readily form hydrogen bonds with nitric acid.[29,30] The presence of these different adsorption sites could also explain why the Langmuir isotherm, which is derived for an energetically homogeneous surface, fits the data poorly. The value of the heterogeneity parameter in the Langmuir−Freundlich isotherm being less than unity would also indicate a heterogeneous surface.

On the other hand, the fact that this heterogeneity parameter is very close to the specific value of 0.5 is strongly suggestive of a reaction mechanism involving dissociation on the soot surface, or else bonding of the nitric acid molecule to neighboring Lewis acid and base sites. The lack of a dependence of the uptakes on relative humidity may simply be a reflection of the relatively small number of water molecules that bind to the soot surface, with binding strengths unable to compete with those of nitric acid to these acid/base sites. Strong, albeit indirect, support for the dissociative mechanism comes from analysis of data published in the literature for SO_2 uptake to *n*-hexane soot.[43] Our analysis of this data set, in the form of a log−log plot of uptake versus SO_2 partial pressure (not shown), is highly linear with a slope of 0.51. Similar behavior for the adsorption of SO_2 to ice has also been observed, where it was hypothesized that SO_2 was dissociating, via reaction with H_2O, to form bisulfite.[33] By contrast, in unpublished work from our laboratory, we have shown that the uptake to soot of species that cannot dissociate, such as benzene, is well fit by the conventional, nondissociative Langmuir isotherm.

We are currently pursuing the use of surface spectroscopic methods to determine more definitively the chemical nature of nitric acid after it binds to the surface.

B. Atmospheric Implications. To determine whether significant quantities of nitric acid will adsorb to soot surfaces in the atmosphere, we need estimates for the amount of soot present and its surface area. For the former, we consider urban polluted conditions of roughly 5×10^{-11} g cm^{-3}, of which up to 10% can be elemental carbon, i.e., 5×10^{-12} g cm^{-3}.[51] Specific surface areas per particulate mass have been measured under urban air conditions to be roughly 2×10^4 cm^2 g^{-1} in two separate studies.[52,53] These measurements were conducted by sampling all particulates onto a filter and then measuring the specific surface area of the collected particles using BET adsorption techniques. This may lead to significant loss of surface area due to coagulation processes, and so these surface area estimates are likely to be a lower limit to what is prevalent in the atmosphere. By contrast, in our work we measured a value of 4×10^5 cm^2 g^{-1} in the linear portion of the plot in Figure 3, i.e., where all the mass was accessible to Kr. Assuming a density of 2 g cm^{-3} and spherical soot particles in our films, this corresponds to an average particle diameter of about 75 nm, not all that dissimilar to the size of the elementary soot particles, i.e., 20−30 nm diameter, that are thought to be part of aggregates in the atmosphere.[51] Using this larger estimate of specific surface area (i.e. 4×10^5 cm^2 g^{-1}) together with the estimate of soot mass (i.e. 5×10^{-12} g cm^{-3}), we arrive at a very rough value of total soot surface area in urban areas to be on the order of 2×10^{-6} cm^2 cm^{-3}.

For a ppbv of gas-phase HNO_3 at ground level (i.e. 7.6×10^{-7} Torr or 2.5×10^{10} molecules cm^{-3}), the surface coverage that we estimate on the soot at room temperature is roughly 5 $\times 10^{11}$ molecules cm^{-2} (see Figure 6). With a total soot surface area of 2×10^{-6} cm^2 cm^{-3}, we estimate that about 1 part in 10^4 of gas-phase nitric acid will be scavenged, i.e., a negligible quantity. This fraction will increase at lower boundary layer temperatures but not to such a degree as to make scavenging by soot an important process for nonreactive removal of gas-phase nitric acid. A similar conclusion can be reached for the conditions of the upper troposphere where surface coverages may be much higher, perhaps even approaching a significant fraction of a monolayer, but total soot surface areas are low. Even though most of our experiments were conducted with dry, "unprocessed" soot, the small dependence of the uptakes on relative humidity and ozone exposure suggests that these conclusions will hold under most atmospheric conditions. The one caveat is, of course, the degree to which our *n*-hexane soot matches that present in the atmosphere.

Even though nonreactive adsorption will lead to little effect on gas-phase nitric acid, it will definitely alter the surficial properties of the soot. This is likely to be significant with respect to the role of soot particles as cloud condensation nuclei and, perhaps, in heterogeneous chemistry. For example, does adsorbed nitric acid react with coadsorbed organics? These effects will be most likely to occur under cold temperatures, where we have shown that significant fractions of a monolayer will be prevalent.

When only nitric acid is present, we are in agreement with most of the recent studies that indicate little irreversible loss of nitric acid when partial pressures are low (and when the surface has not been "activated" by exposure to the flame). In addition, we see no evidence for HONO production, as has been recently reported on soot produced from fuel-rich decane flames.[11] We cannot rule out that irreversible loss of nitric acid was occurring with small uptake coefficients in our flow tube, but long-term experiments conducted in smog chambers suggest that the reactive uptake coefficients for nitric acid can be very low, less than 10^{-7}.[22] However, given the importance of HONO to the atmosphere, we nevertheless plan future experiments, using CIMS detection to see if small yields are prevalent and to investigate the effect of coadsorbed water on the reactive nature of soot.

Acknowledgment. Funding came from NSERC, and also, acknowledgment is made to the Donors of the Petroleum Research Fund administered by the American Chemical Society for partial support of this research. Daniel Aubin would also like to thank Dr. Oleg Sokolov and Dr. Troy Thornberry for their assistance.

References and Notes

(1) Goldberg, E. D. *Black Carbon in the Environment: Properties and Distribution*; Wiley-Interscience: New York, 1985.
(2) Penner, J. E.; Eddleman, H.; Novakov, T. *Atmos. Environ.* **1993**, *27A*, 1277−1295.
(3) *Particulate Carbon: Atmospheric Life Cycle*; Wolf, G. T., Klimisch, R. L., Eds.; Plenum Press: New York, 1982.
(4) Gray, H. A.; Cass, G. R.; Huntzicker, J. J.; Heyerdahl, E. K.; Rau, J. A. *Sci. Total Environ.* **1984**, *36*, 17−25.
(5) Grosjean, D. *Sci. Total Environ.* **1984**, *32*, 133−145.
(6) Horvath, H. *Atmos. Environ.* **1993**, *27A*, 293−317.
(7) Jensen, E.; Toon, O. *Geophys. Res. Lett.* **1997**, *24*, 249−252.
(8) Hallett, J.; Hudson, J. G.; Rogers, C. F. *Aerosol Sci. Technol.* **1989**, *10*, 70−83.
(9) Brown, R. C.; Miake-Lye, R. C.; Anderson, M. R.; Kolb, C. E.; Resch, T. J. *J. Geophys. Res.* **1996**, *101*, 22939−22953.
(10) Schumann, U.; Strom, J.; Busen, R.; Baumann, R.; Gierens, K.; Krautstrunk, M.; Schroder, F. P.; Stingl, J. *J. Geophys. Res.* **1996**, *101*, 6853−6869.
(11) Salgado Munoz, M. S.; Rossi, M. J. *Phys. Chem. Chem. Phys.* **2002**, *4*, 5110−5118.

(12) Hauglustaine, D. A.; Ridley, B. A.; Solomon, S.; Hess, P. G.; Madronich, S. *Geophys. Res. Lett.* **1996**, *23*, 2609−2612.
(13) Singh, H. B.; Herlth, D.; Kolyer, R.; Salas, L.; Bradshaw, J. D.; Sandholm, S. T.; Davis, D. D.; Crawford, J.; Kondo, Y.; Koike, M.; Talbot, R.; Gregory, G. L.; Sachse, G. W.; Browell, E.; Blake, D. R.; Rowland, F. S.; Newell, R.; Merrill, J.; Heikes, B.; Liu, S. C.; Crutzen, P. J.; Kanakidou, M. *J. Geophys. Res.* **1996**, *101*, 1793−1808.
(14) Brown, S. S.; Talukdar, R. K.; Ravishankara, A. R. *J. Phys. Chem. A* **1999**, *103*, 3031−3037.
(15) Finlayson-Pitts, B. J.; Pitts, J. N. J. *Chemistry of the Upper and Lower Atmosphere: Theory, Experiments and Applications*; Academic Press: San Diego, 2000.
(16) Blake, D.; Kato, K. *J. Geophys. Res.* **1995**, *100*, 7195−7202.
(17) Longfellow, C. A.; Ravishankara, A. R.; Hanson, D. *J. Geophys. Res.* **2000**, *105*, 24345−24350.
(18) Choi, W.; Leu, M.-T. *J. Phys. Chem. A* **1998**, *102*, 7618−7630.
(19) Kirchner, U.; Scheer, V.; Vogt, R. *J. Phys. Chem. A* **2000**, *104*, 8908−8915.
(20) Prince, A. P.; Wade, J. L.; Grassian, V. H.; Kleiber, P. D.; Young, M. A. *Atmos. Environ.* **2002**, *36*, 5729−5740.
(21) Rogaski, C. A.; Golden, D. M.; Williams, L. R. *Geophys. Res. Lett.* **1997**, *24*, 381−384.
(22) Saathoff H.; Naumann K. H.; Riemer N.; Kamm S.; Mohler O.; Schurath U.; Vogel H.; B., V. *Geophys. Res. Lett.* **2001**, *28*, 1957−1960.
(23) Disselkamp, R.; Carpenter, M.; Cowin, J. *J. Atmos. Chem.* **2000**, *37*, 113−123.
(24) Kleffmann, J.; Becker, K. H.; Lackhoff, M.; Wiesen, P. *Phys. Chem. Chem. Phys.* **1999**, *1*, 5443−5450.
(25) Pankow, J. F.; Storey, J. M. E.; Yamasaki, H. *Environ. Sci. Technol.* **1993**, *27*, 2220−2226.
(26) Goss, K.-U.; Eisenreich, S. J. *Atmos. Environ.* **1997**, *31*, 2827−2834.
(27) Jang, M.; Kamens, R. M. *Environ. Sci. Techn.* **1998**, *32*, 1237−1243.
(28) Chughtai, A. R.; Smith, D. M.; Kim, J. M. *J. Atmos. Chem.* **2002**, *43*, 21−43.
(29) Akhter, M. S.; Chughtai, A. R.; Smith, D. M. *Appl. Spectrosc.* **1985**, *39*, 143−153.
(30) Akhter, M. S.; Chughtai, A. R.; Smith, D. M. *Appl. Spectrosc.* **1985**, *39*, 154−167.
(31) Akhter, M. S.; Chughtai, A. R.; Smith, D. M. *Appl. Spectrosc.* **1991**, *45*, 653−665.
(32) Chughtai, A. R.; Brooks, M. E.; Smith, D. M. *J. Geophys. Res.* **1996**, *101*, 19505−19514.
(33) Clegg, S. M.; Abbatt, J. P. *J. Phys. Chem. A* **2001**, *105*, 6630−6636.
(34) Brunauer, S.; Emmett, P. H.; Teller, E. *J. Am. Chem. Soc.* **1938**, *60*, 309−319.
(35) Sing, K. S. W.; Everett, D. H.; Haul, R. A. W.; Moscou, L.; Pierotti, R. A.; Rouquerol, J.; Siemieniewska, T. *Pure Appl. Chem.* **1985**, *57*, 603−619.
(36) Alcala-Jornod, C.; van den Bergh, H.; Rossi, M. *Phys. Chem. Chem. Phys.* **2000**, *2*, 5584−5593.
(37) Abbatt, J. P. *Geophys. Res. Lett.* **1997**, *24*, 1479−1482.
(38) Rouquerol, F. *Adsorption by Powders and Porous Solids: Principles, Methodology and Applications*; Academic Press: San Diego, 1999.
(39) Underwood, G.; Li, P.; Usher, C. R.; Grassian, V. *J. Phys. Chem.* **2000**, *104*, 819−829.
(40) Jaroniec, M. R. *Physical Adsorption of Heterogeneous Solids*; Elsevier: Amsterdam, 1998.
(41) Atkins, P. *Physical Chemistry*, 6th ed.; W. H. Freeman and Company: New York, 1998.
(42) Muenter, A.; Koehler, B. *J. Phys. Chem.* **2000**, *104*, 8527−8534.
(43) Koehler, B. G.; Nicholson, V. T.; Roe, H. G.; Whitney, E. S. *J. Geophys. Res.* **1999**, *104*, 5507−5514.
(44) Howard, C. *J. Phys. Chem.* **1979**, *83*, 3−9.
(45) Kemball, C.; Rideal, E. K. *Proc. R. Soc. London Ser. A* **1946**, *187*, 53−73.
(46) Geng, A.; Loh, K.-C. *J. Colloid Interface Sci.* **2001**, *239*, 447−457.
(47) *CRC Handbook of Chemistry and Physics*; 71st ed.; Lide, D. R., Ed.; CRC Press: Boca Raton, FL, 1990.
(48) Alcala-Jornod, C.; van den Bergh, H.; Rossi, M. J. *Geophys. Res. Lett.* **2002**, *29*, 1.1−1.4.
(49) Kamm, S.; Mohler, O.; Naumann, K.-H.; Saathoff, H.; Schurath, U. *Atmos. Environ.* **1999**, *33*, 4651−4661.
(50) Schurath, U.; Naumann, K.-H. *Pure Appl. Chem.* **1998**, *70*, 1353−1361.
(51) Seinfeld, J. H.; Pandis, S. N. *Atmosheric Chemistry and Physics: From Air Pollution to Climate Change*; John Wiley and Sons: New York, 1998.
(52) Sheffield, A. E.; Pankow, J. F. *Environ. Sci Technol.* **1994**, *28*, 1759−1766.
(53) Corn, M.; Montgomery, T. L.; Esmen, N. A. *Environ. Sci. Technol.* **1971**, *5*, 155−158.